High-speed sensing for object detection in underwater bi-static acoustic paths

Angela Digulescu*†, Cindy Bernard*, Elena Lungu†, Ion Candel* and Cornel Ioana*
*University of Grenoble-Alpes, GIPSA-lab, Saint Martin D'Heres, France
Email: [angela.digulescu, cindy.bernard, ion.candel, cornel.ioana]@gipsa-lab.grenoble-inp.fr
†Sigintec, 334 rue Tour de l'Eveque, 30000, Nimes, France
Email: elungu@sigintec.fr

***Abstract*—Detection of objects in underwater environment is an important operation that can be aimed to assess the pollution in the region under study as well as to prevent intrusion of undesired objects in off shore power production facilities or in the restricted entrance area. The use of acoustic methods has been proven to be very powerful for the detection and localization of the underwater objects. This paper proposes a new method for the detection of an underwater object using bi-static acoustic paths. The method uses the dynamic evolution the phase space of the received signals, namely the phase space trajectory, without any synchronization and it computes the point wise Euclidean norm. The detection map obtained gives both the amplitude and time of arrival information. The major advantage brought by this approach (rather than conventional techniques) is that the signals need no synchronization, their characterization being based only on their wave form.**

Keywords*—phase space; recurrence matrix; detection curve; time of arrival

I. Introduction

Underwater object detection is an important task for the marine community and it represents a heavy duty for the signal processing field. Its purpose can relate to the monitoring of the underwater fauna as least intrusive as possible, as well as to supervise the pollution in the studied area.

While the detection part has been studied using various methods like correlation techniques [1], time-frequency methods [2], sonar imaging [3], etc., our approach is based on high speed sensing in order to determine the time of arrival (TOA) of the object relative to a reference response. This implies that there is no synchronization between the emission and reception. Moreover, our approach also proposes to characterize the trajectory of the object.

Therefore, the application is based on a wide-band active acoustic system, these types of signals being more robust to on-site drawbacks like: ambient noise, electronic noise, interference sources, etc. [2]. Then, the TOAs are determined using the Recurrence Plot Analysis (RPA) method. The method is applied for each response of a fixed length and the result is stored in a detection map which contains the time bins of the responses and the time distributed recurrences (TDR) computed for each time bin. Next, the TOAs of each response are determined relative to the first one and a comparison with the classical signal envelope approach is done.

The paper is organized as follows: in section II, the RPA method will be presented; section III will describe the experimental setup and in section IV, the results are highlighted. Then, in section V, the most important ideas and future work aspects are presented.

II. Recurrence Plot Analysis method

The Recurrence Plot Analysis (RPA) is derived from the dynamical systems theory and it considers the evolution of a measurement in its phase space [4], [5]. Therefore, we firstly consider a received signal as the time series [6], [7] expressed in (2):

$$\mathbf{x} = \{x[1], x[2], ..., x[N]\} \tag{1}$$

where N is the length of the received signal.

Then, the time series is represented in a m dimensional phase space. The vectors that describe the trajectory of the dynamical system have as coordinates m values of the time series which equally spaced:

$$\vec{v_i} = \sum_{k=1}^{m} x[i + (k-1)d] \cdot \vec{e_k}, i = \overline{1, M} \tag{2}$$

where $\vec{v_i}$ are the vectors from the phase space corresponding to a state of the system, m is the embedding dimension, d is the the delay (lag) between the samples of the received signal, $M = N - (m-1)d$ and $\vec{e_k}$ are the axis unit vectors.

Afterwards, the next step of the RPA method is to compute the distance/ recurrence matrix. The distance matrix determines the pointwise distance between the points of the phase space. These points are given by the position vectors expressed in (2):

$$D_{i,j} = \Delta(v_i, v_j) \tag{3}$$

$$R_{i,j} = \Theta(\varepsilon - \Delta(v_i, v_j)) \tag{4}$$

where $\Delta(v_i, v_j)$ from (3) is a distance considered between the points from the phase space (the Euclidean distance, the L_1 norm, the angular distance [7], etc.). The operator $\Theta(\cdot)$ from (4) is the Heaviside step function and $\varepsilon(\cdot)$ is the chosen threshold that discriminates if one distance is a states of recurrence or not (usually is value is constant).

The most important parameters of the RPA method are the delay, d and the embedding dimension, m. The choice of the delay [8] is critical for the "quality" of the trajectory in the phase space. If the delay is chosen too small, then the trajectory is over folded around the main diagonal of the phase space, hereby the representation is redundant. But, if the delay is

978-0-933957-43-5 ©2015 MTS

too large, the phase space evolution of a measured time series could appear very complicated in the presence of noise, thus the representation is irrelevant. Therefore, the proper value of this parameter is chosen based on the independence of the time series samples. Therefore, among the proposed methods, the most used method for the proper estimation of the delay is the mutual information method [7]. A well suited value of the delay is the value for which the mutual information is small enough, but not zero:

$$I_{AB} = \log_2 \left(\frac{P_{AB}(a_i, b_j)}{P_A(a_1) \cdot P_B(b_j)} \right) \quad (5)$$

where $P_A(a)$ is the probability of having the a value by measuring the A system and $P_{AB}(a, b)$ is the probability of having simultaneously the a value by measuring the A system and the b value from the B system. In theory [6], [8], the optimal choice of the delay is given by the value corresponding to the first local minimum of the mutual information.

The second most important parameter of the method is the embedding dimension, m. Its choice is based on the following idea: let m_0 be the actual dimension of the phase space; if the trajectory is represented in an m_1 dimension (where $m_1 < m_0$), then this representation is just a projection of the actual trajectory and some point would appear close to others, whereas in the m_0 dimension they would not be neighbours. If the choice of the embedding dimension is larger than m_0, for a long time series, higher computational resources would be required. Using the idea previously presented, usually the choice of the dimension is achieved with the False Nearest Neighbor method [6], [9].

The link between the distance matrix and the recurrence matrix is represented by the threshold, ε. This parameter can be interpreted in two ways: in the phase space is a certain neighbourhood of radius ε (if ε is constant in $2D$, then the neighborhood is a rhombus for the L_1 norm and a circle for the Euclidean distance); on the distance matrix, the threshold represents a horizontal section of a landform, where the landform are the distances from the matrix; hereby, on the recurrence matrix is obtained, the values of the distances matrix under the ε value are considered as recurrent and have the value 1 (generally plotted in black), and the values above the threshold are considered distant and are equal to 0 (usually represented in white).

For the detection of the object's response, the detection map is obtained from the recurrence matrix. Each line from the detection map represents the time distributed recurrences (TDR) of a fixed time bin of the object's response. The TDR measure highlights the exitance of a sudden change that is totally different from all others in the phase space, as well as on the recurrence matrix [7], [8]. In [7], it was proven that even with a weak signal to noise ratio, the sudden change of the system's state is pointed out through a white horizontal/ vertical line on the recurrence matrix. Considering this characteristic, we defined in [7] the time distributed recurrence measure which can be interpreted as a time average distance:

$$TDR(l) = \sum_{i=1}^{M} R_{i,l}, l = \overline{1, M} \quad (6)$$

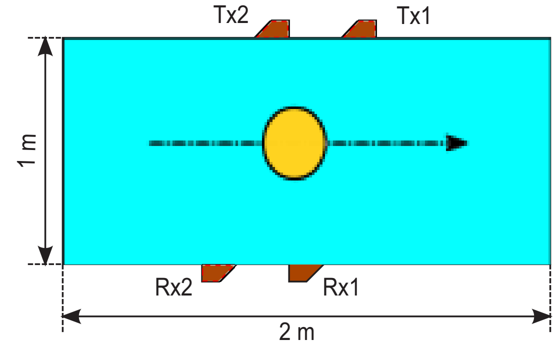

(a) The experimental facility

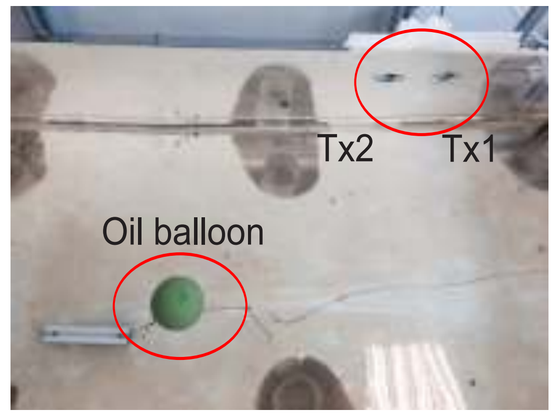

(b) The on-site set-up

Fig. 1: The experimental configuration: the dash-dot line shows the trajectory of the object

In order to point out the sudden change from the time series, we usually use the complementary version of the TDR measure (6):

$$TDR^*(l) = 1 - \frac{TDR(l)}{\max(TDR(l))} \quad (7)$$

Considering that the passage of the object in front of the sensors, involves a change in the received time series, we aim to highlight this effect on the detection map based on the TDR^* measure (8). Hereby, we define the detection map:

$$DM(l, \tau) = [TDR^*(l)]_{\tau = \overline{1, \frac{N}{s}}} \quad (8)$$

where N is the length of the recorded signal and s is the size of the fixed time bin for which the TDR^* measure is computed.

The detection map contains both the amplitude (in the TDR^* measure) and time of arrival information (given by the time bin, τ). Therefore, this approach presents the time information, although the signals have no synchronization and their characterization is based only on the received signals at the two sensors.

III. Experimental setup

The experiment was performed on a reduced scale facility where the underwater object travelled for $3s$ on a distance of $1.5m$. The underwater object was an oil balloon entirely

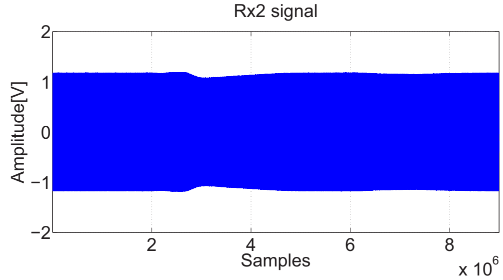

Fig. 2: The recorded signal arrived at $Rx2$ sensor

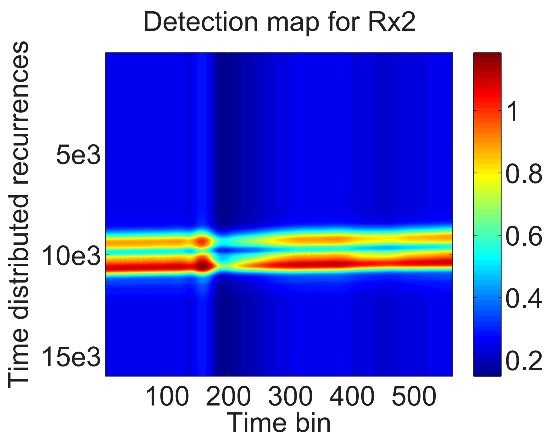

Fig. 3: The detection map obtained for the $Rx2$ signal

immersed, intersecting the acoustic paths upon moving. The experimental configuration is presented in figure 1.

All four acoustic transducers are identical and have a wide band reception centred on $1MHz$ with a bandwidth that starts from $800kHz$ and ends around $1200kHz$. The output signal varies from $-10V$ to $10V$. The emission transducers ($Tx1$ and $Tx2$) are placed on one side of the water tank and continuously generate linear chirp burst in their bandwidth at an angle of $45°$. On the opposite side of the water tank, the receiving sensors are placed at a minimum distance such that cross-talk between the acoustic paths is avoided in the clear water (when no object is in the water tank). The data acquisition is performed for a duration of approximately $3.35s$ in order to record the entire process.

IV. Results

Taking into account that each received signal has over $33million$ samples, we have processed only the part of the signal corresponding to passage of the balloon in front of the sensors. This observation reduces its computational time at a third of its actual time.

For the detection part, we present only the signal recorded at $Rx2$ (fig. 1a) sensor which directly receives its bursts from $Tx2$. On this signal, fig. 2, the detection map based on the TDR^* measure is applied, fig. 3.

It can be observed that the burst (the response of the object) is represented by the two brown horizontal lines which vary in amplitude (the average distance on the phase space changes),

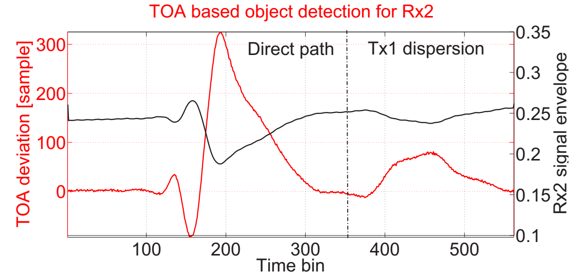

Fig. 4: The TOAs (red) of each response of $Rx2$ signal and its signal envelope (black)

but also in time (the TOAs of the bursts in each time bin is not constant). Moreover, as the lines of the detection map (8) represent the value of the TDR^* measure in each time bin, its columns contain the information regarding the TOAs of each burst in its corresponding time bin.

Therefore, in order to obtain the TOA information from the detection map (fig. 3), we impose an appropriate threshold that discriminates between the the part of the signal that has no burst and the one that has it. In this case, the threshold is given by the cyan region from the detection map. Hereby, the first point on each column of the detection map corresponding to the cyan region gives the TOA of the responses in in each time bin. The results are presented in fig. 4.

Although, the signal's envelope does not offer reliable information regarding the object (the amplitude variation can be caused by external vibrations, move of transducers, etc.), the TOA information is very robust, because it highlights the delay induced by the object. From fig. 4 it can be seen that, even for a slight attenuation in signal's amplitude, the detection map approach is able to highlight a delay in the TOA of the burst for two time bin intervals.

This delay is explained by the fact that the speed of sound in the sunflower oil is smaller (around $1425m/s$) than the water speed of sound (around $1480m/s$) and its maximum corresponds to the delay induced by the oil ball diameter ($15cm$) and the rubber wall ($0.5mm$) of the balloon that folds the oil ball.

Moreover, on the TOA based object detection representation, the first interval corresponds to the object passing in front of the transducer $Tx2$ and the second corresponds to the cross-talk induced by the dispersion of signals coming from $Tx1$. In this way, we suppose that the travel direction of the object is from $Tx2$ to $Tx1$. In order, to confirm our assumption, we also study the signals recorded by $Rx1$ (fig. 5).

In this case, the signal is more disturbed in terms of amplitude. Figures 6 and 7 present the detection map corresponding to the $Rx1$ signal and the TOAs of the responses from each time bin. It seems that even that the amplitude of the signal is more disturbed, its TOAs present almost the same values for the positives peaks.

The TOA representations from fig. 4 and 7 point out approximately the same maximum delays induced by the object. This observation leads to the conclusion that one and the same object has passed in front of the sensors. Furthermore, the other

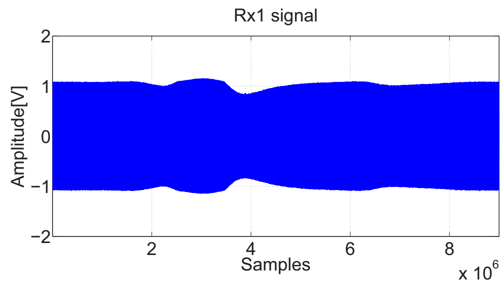

Fig. 5: The recorded signal arrived at $Rx1$ sensor

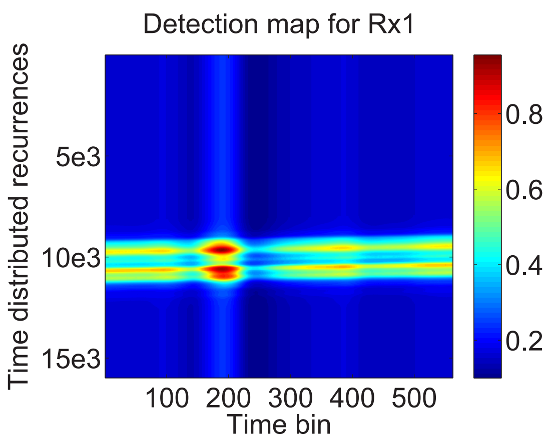

Fig. 6: The detection map obtained for the $Rx1$ signal

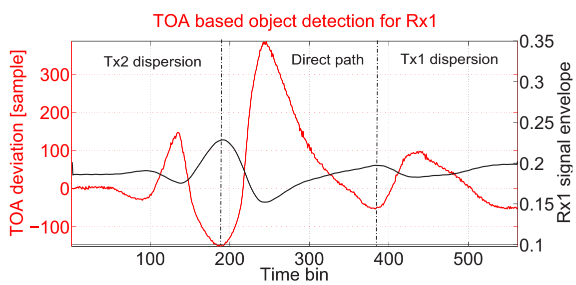

Fig. 7: The TOAs (red) of each response of $Rx1$ signal and its signal envelope (black)

variations of the TOAs are caused by the crosstalk that the signals' dispersion in the balloon induces to the sensors. We recall that, in the configuration with no object in the water, the sensors were placed at a minimum so that they record only the response coming from their corresponding transceiver ($Tx2-Rx2$ and $Tx1-Rx1$, respectively). But, in the presence of the object, its movement induces a cross-talk between the sensors.

In fig. 4, two peaks can be observed: a maximum which automatically corresponds to de delay induced by the object that interferes with the direct path between the pair $Tx2-Rx2$, and the second peak corresponds to the cross-talk induced by $Tx1$ as the object travels towards its path. Also, in fig. 7, three peaks are present: the maximum which corresponds to the passing of the object through the direct path between $Tx1-Rx1$, a second peak present before the maximum which is caused by the reflections coming from $Tx2$ and a third peak caused by the reflections of $Tx1$. These observations lead to the conclusion that the object moves from left to right in the given configuration.

V. Conclusion

This paper proposes a new method for the detection of an underwater object using bi-static acoustic paths. The main advantage of the RPA method is that it uses only the signals arrived at reception (so there is no synchronization). Starting from the fact that a sudden change in the signal is easily highlighted by the TDR^* measure [7], we define the detection map based on this measure. This map contains both amplitude and time information. The latter is obtained in terms of a fixed time bin which is chosen according to our application.

Applying our method on the signal arrived at one of the sensors, we point out the presence of the underwater object from the TOA information which is very robust, because it highlights the delay induced by the object, although the signal's envelope is not that reliable. Moreover, the information given by the second sensor adds up extra information, confirming that, in the water tank, there is only one object and that it moves from left to right.

Future work foresees the detection and characterization of multiple underwater objects based on the high-speed sensing.

Acknowledgment

This work has been funded by the FUI-Tenerrdis project "Smart Hydro Monitoring".

References

[1] Y. Chunhua, M. R. Azimi-Sadjadi, J. Wilbur and G. J. Dobeck, "Underwater target detection using multichannel subband adaptive filtering and high-order correlation schemes", IEEE J. Ocean. Eng., vol. 25, no. 1, pp. 192-205, 2000.

[2] A. Digulescu, I. Candel, F. Bunea, D. Bucur, C. Ioana and T. Petrut, "Underwater object tracking using time-frequency signatures of acoustic signal", OCEANS'14 MTS/IEEE Conference, Taipei, Taiwan, 2014.

[3] S. Xie, J. Chen, J. Luo, P. Xie and W. Tang,"Detection and Tracking of Underwater Object Based on Forward-Scan Sonar", Intelligent Robotics and Applications, Lecture Notes in Computer Science, vol. 7506, pp. 341-347, 2012.

[4] N. Packard, J. Crutchfield, D. Farmer and R. Shaw, "Geometry from a time series", Physical Review Letters, vol. 45(9), pp. 712-716, 1980.

[5] J. P. Eckmann, S. O. Kamphorst, D. Ruelle, "Recurrence Plots of Dynamical Systems", Europhysics Letters, vol. 5(9), pp. 973-977, 1987.

[6] N. Marwan, S. Schinkel, J. Kurts, "Recurrence plots 25 years later Gaining confidence in dynamic transitions", Europhysics Letters, 101, 20007, 2013.

[7] C. Ioana, A. Digulescu, A. Serbanescu, I. Candel, F.M. Birleanu, "Recent Advances in Nonstationary Signal Processing Based on the Concept of Recurrence Plot Analysis", Springer Proc. in Mathematics & Statistics, M. Marwan et al. (Eds.): "Translational Recurrences", pp. 75-93, Cham, Switzerland, 2014.

[8] I. Candel, A. Digulescu, C. Ioana, A. Serbanescu, E. Sofron, "Optimization of partial discharge detection in high voltage cables based on advanced signal processing techniques", The 11th Conference on Information Science, Signal Processing and their Applications, ISSPA 2012, Montreal, Canada, July, 2012.

[9] M. Small, "Applied nonlinear time series analysis. Applications in phisiscs, physiology and finance", World Scientific Publishing, New Jersey, 2005.